The Bowen Ratio of an Alpine Grassland in Three-River Headwaters, Qinghai-Tibet Plateau, from 2001 to 2018

Authors: Xuanlan, Zhao, Junbang, Wang, Hui, Ye, Amir, Muhammad, and Shaoqiang, Wang

Source: Journal of Resources and Ecology, 12(3) : 305-318

Published By: Institute of Geographic Sciences and Natural Resources Research, Chinese Academy of Sciences

URL: https://doi.org/10.5814/j.issn.1674-764x.2021.03.001

J. Resour. Ecol. 2021 12(3): 305-318
DOI: 10.5814/j.issn.1674-764x.2021.03.001
www.jorae.cn

The Bowen Ratio of an Alpine Grassland in Three-River Headwaters, Qinghai-Tibet Plateau, from 2001 to 2018

ZHAO Xuanlan[1,2], WANG Junbang[1,*], YE Hui[3], MUHAMMAD Amir[1,2], WANG Shaoqiang[1]

1. National Ecosystem Science Data Center, Key Laboratory of Ecosystem Network Observation and Modeling, Institute of Geographic Sciences and Natural Resources Research, Chinese Academy of Sciences, Beijing 100101, China;
2. University of Chinese Academy of Sciences, Beijing 100049, China;
3. College of Tourism and Geography, JiuJiang University, Jiujiang, Jiangxi 332005, China

Abstract: The Bowen ratio (β) is used to quantify heat transfer from the land surface into the air, which is becoming a hot topic in research on the biogeophysical effects of land use and cover changes. The Three-River Headwaters (TRH), as a sensitive and fragile region, was selected as the study area. The β for 2001–2018 was estimated from the evapotranspiration product (ET_{MOD16}) of MODIS and the net radiation of the land surface through the albedo from GLASS. The ET_{MOD16} data were evaluated against the observation data (ET_{OBS}) at two alpine grassland flux towers obtained from ChinaFLUX. The interannual trend of the β was analyzed by multiple linear regression (MLR) and structure model (SEM) with the multiple factors of precipitation, temperature, humidity, albedo, and normalized difference vegetation index (NDVI, MOD09Q1). The results show that the ET_{MOD16} values were significantly correlated with ET_{OBS}, with a correlation coefficient above 0.70 ($P < 0.01$) for the two sites. In 2001–2018, the regional mean β was 2.52 ± 0.77 for the whole grassland, and its spatial distribution gradually increased from the eastern to western region. The interannual β showed a downward trend with a *slope* of −0.025 and a multiple regression coefficient (R^2) of 0.21 ($P = 0.056$). Most of the variability (51%) in the interannual β can be explained by the linear regression of the above multiple factors, and the temperature plays a dominant role for the whole region. The SEM analysis further shows that an increasing NDVI results in a decreasing albedo with a path coefficient of −0.57, because the albedo was negatively correlated with NDVI ($R^2 = 0.52$, $P < 0.01$), which indicates a negative and indirect effect on β from vegetation restoration. An obvious warming climate was found to prompt more evapotranspiration, and restoring vegetation makes the land surface receive more radiation, which both resulted in a decreasing trend in the annual β. This study revealed the biogeophysical mechanisms of vegetation restoration under a changing climate, and demonstrated the Bowen ratio can be applied as an indicator of climate-regulating functions in ecosystem assessments.

Key words: alpine grassland; Bowen ratio; Three-River Headwaters; MODIS; evapotranspiration

1 Introduction

Terrestrial ecosystems are both driven by and exert impacts on climate (Bonan, 2008, 2017). Land use, degradation, or restoration will change the physical properties of the ecosystem, such as albedo, leaf area index (LAI), and roughness length, which further alters the exchanges of energy and water fluxes between the ecosystem and the atmosphere, with consequent impacts on the local and regional climate.

Received: 2020-08-02 **Accepted:** 2020-10-20
Foundation: The National Key Basic Research and Development Program (2017YFC0503803); The National Natural Science Foundation of China (31971507); Qinghai Province Science and Technology Program (2018-ZJ-T09); CAS-Qinghai Province Joint Program on Three-River Headwaters National Park (YHZX-2020-07).
First author: ZHAO Xuanlan, E-mail: zhaoxl.17s@igsnrr.ac.cn
***Corresponding author:** WANG Junbang, E-mail: jbwang@igsnrr.ac.cn

Citation: ZHAO Xuanlan, WANG Junbang, YE Hui, et al. 2021. The Bowen Ratio of an Alpine Grassland in Three-River Headwaters, Qinghai-Tibet Plateau, from 2001 to 2018. *Journal of Resources and Ecology*, 12(3): 305–318.

The effects of land-use changes have been widely studied (Betts, 2000; Cao and Li, 2000; Pielke et al., 2002; Feddema et al., 2005). To the best of our knowledge, however, the effects of land degradation and restoration on energy exchange have rarely been investigated in previous studies.

Grassland degradation and restoration have occurred on the Qinghai-Tibet Plateau, so it is an ideal location for determining the effects of land-use changes. Three-River Headwaters (TRH), located in the hinterland of the Qinghai-Tibet Plateau, is known as the water tower for the whole of China, and even for all of Southern Asia, because it includes the headwaters of the Yangtze, Yellow, and Lancang Rivers (Mei, 2000). In TRH, the Alpine grassland has been suffering from degradation since the 1970s, and the degraded area was 36.12% of the total grassland and continued to increase by a rate of 3.87% between 1990 and 2004 (Liu et al., 2008). Since 2005, many ecological measures have been implemented to restore the grassland and its degradation has been controlled to some extent (Shao et al., 2013; Shao et al., 2017; Huang et al., 2018). Meanwhile, the evapotranspiration of the grasslands increased significantly across the Qinghai-Tibet Plateau from 1982 to 2014 (Cui et al., 2019), which means that the latent heat has increased. Our previous analysis for the region showed a significantly warming and wetting climatic trend in the interpolated meteorological data in 1990–2012 (Yang et al., 2019) and an insignificant greening trend in the remote sensing-based normalized difference vegetation index (NDVI) since 2000 to 2015 (Wang et al., 2019). These findings raised the question of how the albedo, net radiation, and Bowen ratio will change with the greening vegetation and increasing latent heat under the background of the impacts of grassland degradation and restoration. The answer to this question will help us to better understand the processes and mechanisms of land degradation and restoration as two kinds of land-use change.

The energy exchanges were mainly determined through three methods, including on-ground observations, process-based modeling, and remote sensing-based estimations. The first method estimates the energy exchanges based on the Bowen ratio/energy balance (BREB), which requires the measurements of temperature and humidity at two levels, net radiation and soil heat flux (Dugas et al., 1991; Zhang et al., 2006; Zhang et al., 2017; Wang et al., 2018). For the second method, the process-based model describes the processes of the water cycle, energy exchange, carbon cycle, and numerous other biogeophysical and biogeochemical processes to capture the various land–atmosphere interactions (Bastiaanssen, 2000; Zhao and Li, 2015; Hao et al., 2016). The third method relies on remote sensing to retrieve some variables in BREB, such as land surface temperature and leaf area index (Liu et al., 2003; Geli et al., 2010). As remote sensing can provide continuous spatial–temporal information on vegetation and surface temperature, the remote sensing-based method has been widely applied. For example, the evapotranspiration products (MOD16) of the moderate resolution imaging spectroradiometer (MODIS) could be classified for the third method; these products have a 1 km spatial resolution and an 8-day time step from 2000 to the present, and are considered to have high accuracy (Mu et al., 2007; Mu et al., 2011).

Therefore, this study applied the newest evapotranspiration product (MOD16 C006) to analyze the spatial–temporal changes in the Bowen ratio and its impacting factors from climate and vegetation in the Three-River Headwaters region. We aimed to gain an understanding of the effects of ecosystem degradation and restoration on the local climate. With developments in ecosystem quality assessment (Wang et al., 2019), the second aim of this study is to provide a methodological reference for the monitoring and assessment of the climate-regulating function of the terrestrial ecosystem.

2 Data and methods

2.1 Overview of the study area

Three-River Headwaters (TRH) is located in Qinghai Province on the Qinghai-Tibet Plateau, with geographic co-ordinates from 31°39′ to 36°12′N and from 89°45′ to 102°23′E, and an altitude from 3335 to 6564 m (Fig. 1). The TRH region serves as the headwaters of the Yangtze River (YTR), Yellow River (YLR), and Lancang River (LCR), with the respective basin areas covering 46%, 28%, and 10% of the total TRH area (Shao and Fan, 2012). It has a typical highland continental climate, with an annual mean temperature from −18.96 to 7.18 ℃ and annual total precipitation from 208.58 to 845.26 mm according to the meteorological data from 2000 to 2018. The dominant vegetation of the study site is alpine grassland.

2.2 Data and processing

2.2.1 Evapotranspiration data

In this study, the land surface Bowen ratio was calculated from the land surface energy balance based on the remote sensing-based evapotranspiration (ET) data. The ET data were obtained from the MODIS product of MOD16A2 C006 with an 8-day temporal resolution and a 500 m spatial resolution for the period from 2001 to 2018 (https://earthdata.nasa.gov/). The algorithm of the MOD16 product is based on the Penman–Monteith equation (Mu et al., 2011):

$$\lambda ET = \frac{s \times R_n + \rho C_p \times \left(e_{sat} - e_a\right) / r_a}{s + \gamma \times \left(1 + r_s / r_a\right)} \quad (1)$$

where λET is latent heat, s is the slope of the relationship between saturation vapor pressure and temperature (Pa ℃$^{-1}$); R_n is net radiation; ρ is air density and C_p is constant pressure specific heat (J kg^{-1} ℃$^{-1}$); e_{sat} is saturated water pressure and e_a is actual water vapor pressure; r_a is air resistance; γ is the humidity constant; and r_s is canopy resistance. The

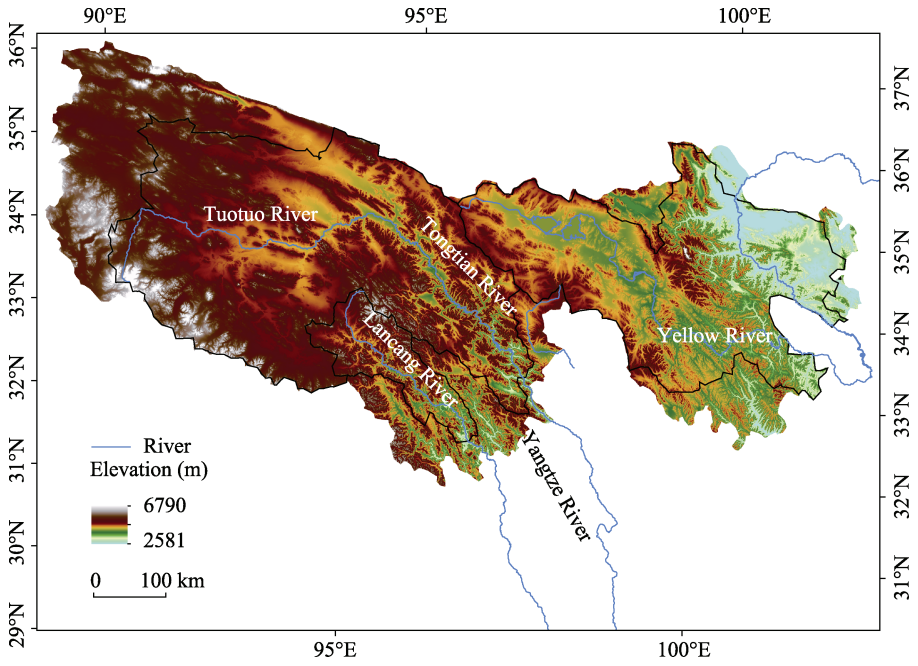

Fig. 1 Location of the Three-River Headwaters Region, Qinghai Province, China.

algorithm was improved by considering vegetation transpiration, vegetation canopy wet surface evaporation, and soil evaporation (Mu et al., 2011):

$$\lambda ET=\lambda ET_{WET\_C}+\lambda ET_{trans}+\lambda ET_{soil} \quad (2)$$

where, λ is Latent heat transfer coefficient; ET is surface evapotranspiration; ET_{WET_C} is evapotranspiration from the wetted canopy, ET_{trans} *is* evapotranspiration from the canopy, and ET_{soil} is evapotranspiration from the soil surface.

2.2.2 Net surface radiation data

The net surface radiation was estimated from the solar shortwave radiation and the albedo data was derived from remote sensing, which was developed in the GLOPEM-CEVSA model (Wang, 2007):

$$R_n = R_{ns} + R_{nl} \quad (3)$$

$$R_{nl}=\sigma T_s^4\left(0.56-0.079\sqrt{e_a}\right)\left(0.10+0.90\frac{n}{N}\right) \quad (4)$$

$$R_{ns} = S\downarrow(1-r)+(\varepsilon L\downarrow-\varepsilon\sigma T_s^4) \quad (5)$$

where, R_n is the net surface radiation; R_{ns} is the shortwave net radiation; R_{nl} is the long-wave net radiation; $S\downarrow$ is the downward short-wave radiation; r is the surface albedo; ε is the surface emissivity; $L\downarrow$ is the downward long-wave radiation; T_s is the surface temperature; σ is Stephen Boltzmann's constant; e_a is actual water vapor pressure; n is actual sunshine hours; and N is reasonable sunshine hours. For detailed calculations, see Wang (2007).

2.2.3 Meteorological data

The meteorological data were obtained from the China Meteorological Science Data Sharing Network (http://date.cma.cn/), including daily precipitation, maximum and minimum temperatures, relative humidity, wind speed, and hours of sunshine observed at meteorological stations in the study area and surrounding area. After a quality check and temporal interpolation of the missing data for a given time series in a given year (to provide a missing values rate of no more than 10%), the meteorological grid data (MeteoGrid) were interpolated through ANUSPLIN software (Hutchinson, 1991, 1998a, 1998b) with the digital elevation model data from SRTM of 90 m spatial resolution (Zhu et al., 2013) as a covariate. The interpolated MeteoGrid data have a spatial resolution of 250 m and a time step of eight days, to match with the MODIS data. The interpolated data were validated against the observed temperature and precipitation data from the seven eddy covariance towers. The data were significantly correlated with the observations and could explain 67% and 94% of the temporal variability in the observed precipitation and temperature data, respectively (Wang et al., 2017).

2.2.4 Observed latent heat data used for validation

The observed latent heat flux data from the two sites of ChinaFlux were used to validate the evapotranspiration product of MODIS (MOD16). The two sites were the alpine shrub at Haibei (101°20′E, 37°40′N, and 3190 m above sea level) and the alpine meadow at Dangxiong (91°03′E, 30°29′N, and 4300 m above sea level). The data were processed by a consistent method for all observations at the ChinaFLUX sites (Yu et al., 2006; Yu et al., 2008; Yu et al., 2014).

2.2.5 The data of vegetation index and surface albedo

The normalized difference vegetation index (NDVI) and land surface albedo data were both from MODIS for the period from 2001 to 2018. The NDVI data were calculated

from the band reflectance data product of MODIS (MOD09Q1) of 250 m spatial resolution, and the spikes in the time series were removed through the Savitzky-Golay (SG) filtering algorithm in Timesat software (Jönsson and Eklundh, 2004). The albedo data were from the GLASS dataset with 1km spatial resolution that is based on a direct-estimation algorithm (Liu et al., 2013a; Liu et al., 2013b; Qu et al., 2014), and they were spatially resampled to a spatial resolution of 250 m.

2.2.6 Digital Elevation Model (DEM)

The DEM data were derived from the 90 m spatial resolution SRTM (Shuttle Radar Topography Mission) dataset produced jointly by the National Aeronautics and Space Administration (NASA) and the National Institute of Mapping (NIMA) of the Ministry of Defense, and they were resampled to a spatial interpolation of 250 m.

2.3 Calculation of the Bowen ratio and analysis methods

2.3.1 Calculation of the Bowen ratio

The Bowen ratio (Bowen, 1926) is defined as the ratio of sensible heat to latent heat (Equation 6). In this study, it is calculated from the net surface radiation and the evapotranspiration-based latent heat according to the surface energy balance (Equation 7).

$$\beta = \frac{H}{\lambda ET} \tag{6}$$

$$R_n = H + \lambda ET + G \tag{7}$$

where, β is Bowen ratio; R_n is the net radiation flux estimated from the remote sensing-based albedo; H is the sensible heat flux estimated as the difference between the R_n and the latent heat flux; and λET is estimated from the evapotranspiration of MOD16 because the soil heat flux G could be ignored due to the small variability of the intra-annual fluctuations.

2.3.2 Analysis method on impacts from multiple factors

Multiple linear regression analysis was applied to quantify the impacts from climatic and vegetation changes on the Bowen ratio through the following equation:

$$\beta = b_0 + b_P P_{AT} + b_T T_{AM} + b_H RH_{AM} + b_A A_{AM} + b_N N_{AM} \tag{8}$$

where, β is the Bowen ratio; P_{AT}, T_{AM}, RH_{AM}, A_{AM} and N_{AM} are the annual total precipitation, the annual mean temperature, annual mean relative humidity, annual mean Albedo and annual mean normalized difference vegetation index, respectively. The terms b_P, b_T, b_H, b_A and b_N are the normalized regression coefficients which characterize the sensitivity of the Bowen ratio to the changes of the P_{AT}, T_{AM}, RH_{AM}, A_{AM} and N_{AM}, respectively, and b_0 is the intercept. The multiple correlation coefficient R^2 of the regression equation and the significance level were applied to determine the performance of the fitted regression equation. The data were normalized in order to compare the relative contributions of the different independent variables.

2.3.3 Structural Equation Model (SEM)

Structural Equation Model (SEM) is a statistical method for analyzing the direct and indirect effects of independent variables on a dependent variable based on the correlation coefficient or covariance matrix between the variables; the main methods commonly used in SEM include path analysis, validation factor analysis, latent variable structural model, growth curve model, etc. (Hua and Cheng, 1999; Shipley, 2000; McDonald and Ho, 2002). Here, the path analysis to resolve the effects of T_{AM}, P_{AT}, RH_{AM}, A_{AM}, and N_{AM} on the Bowen ratio was performed using the Lavaan package (Rosseel, 2012) in the *R* language, which does not require potential variables. Firstly, the correlation analysis is performed by the GGally package ggcorr function of the *R* language to determine the correlation between the independent variables, and then the following correlations (Equations 9 to 13) were considered to analyze the direct and indirect effects of the independent variables on the Bowen ratio by the path analysis function in the lavaan package.

$$N_{AM} \sim T_{AM} + P_{AT} + RH_{AM} \tag{9}$$

$$\beta \sim T_{AM} + P_{AT} + RH_{AM} + A_{AM} + N_{AM} \tag{10}$$

$$T_{AM} \sim P_{AT} \tag{11}$$

$$A_{AM} \sim T_{AM} + P_{AT} + N_{AM} + RH_{AM} \tag{12}$$

$$RH_{AM} \sim T_{AM} + P_{AT} \tag{13}$$

3 Results and analysis

3.1 Changes of climate and vegetation

The interannual changes from 2000 to 2018 of the annual total precipitation (P_{AT}), the annual mean temperature (T_{AM}) and NDVI (N_{AM}) for the whole region and the three sub-basins in Three-River Headwaters were shown in Fig. 2. According to the multi-year averaged values, the annual total precipitation was 484.19 ± 130.43 mm, the annual mean temperature was –3.33 ± 2.39 ℃, the annual mean humidity was 56.27% ± 4.66%, the annual mean NDVI was 0.19 ± 0.11, and the annual mean albedo was 0.22 ± 0.04 for the whole region.

During the period 2000–2018, the climatic changes showed insignificant wetting but significant warming trends, with increasing rates of 29.7 mm per decade (P = 0.20) for the P_{AT}, and 1.0 ℃ per decade (P < 0.01) for the T_{AM}, respectively. The vegetation was greening by 0.6% per decade (P = 0.05), while the A_{AM} was decreasing by 1% per decade (P = 0.04).

The climatic changes and vegetation responses varied among the three basins of the Yellow River, Yangtze River and Lancang River. The trends of precipitation were insignificant, with slopes of 14.02 mm, 45.05 mm and 0.37 mm per decade and significance levels (P) of 0.09, 0.41, and 0.62, respectively, for the three basins. However, the temperatures showed significant warming trends, with slopes of

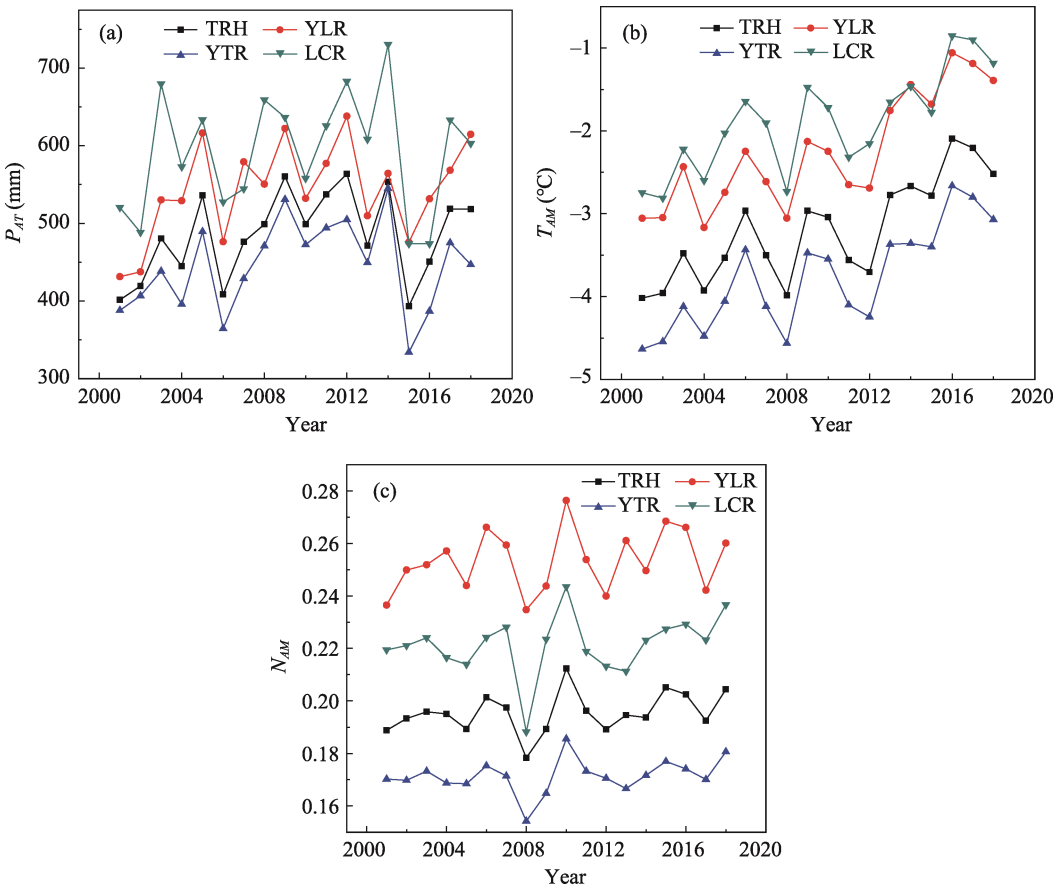

Fig. 2 Interannual changes of the annual total precipitation (P_{AT}), the annual mean temperature (T_{AM}) and NDVI (N_{AM}) of the whole region (TRH) and the three sub-basins of Yellow River (YLR), Yangtze River (YTR) and Lancang River (LCR) in the Three-River Headwaters, Qinghai, China, from 2000 to 2018.

1.02 ℃, 1.14 ℃ and 0.98 ℃ per decade and the P values were less than 0.001 for each of the three basins. These results indicated that the whole region experienced a warming climate, and the Yellow River Basin had a warming and wetting climate.

The trends of the NDVI were also insignificant, but they were increasing at rates of 0.5%, 0.8% and 0.7% per decade for the three basins. In contrast, the albedo showed a decreasing trend in each basin, with the rates of –1.3%, –1.2% and –1.1% per decade, which meant that more solar radiation would be absorbed by the land surface according to Equation 4 along with the greening of vegetation in that region.

3.2 Evapotranspiration validation

The data were sampled for the 3×3 pixel areas centered around the eddy covariance towers in the MOD16A2 products (ET_{MOD16}), and the mean of the data was compared with the observations (ET_{OBS}) for the eddy covariance towers at Haibei and Dangxiong grasslands. The results showed that the ET_{MOD} was significantly correlated with the ET_{OBS}, and the multiple correlation coefficients were 0.61 and 0.45 for the two sites respectively, each with a P value of less than 0.01; which indicated the MOD16 product could explain 61% and 45% of the seasonal changes in the observations and could capture the seasonal changes in the ET of the alpine grass reasonably well, although some underestimations were found as shown by the RMSE of 6.44 and 8.19 mm m^{-2} $(8\ day)^{-1}$ at Haibei and Dangxiong, repectively (Fig. 3).

3.3 Bowen ratio and its spatio-temporal changes

3.3.1 Energy exchanges and Bowen ratio

Figure 4 shows the Bowen ratio, latent heat, net radiation, and sensible heat in the Three-River Headwaters region for the period from 2001 to 2018. The net surface radiation was 3304.73 ± 342.79 MJ m^{-2} yr^{-1} with the latent heat flux from the MOD16A2 C006 of 980.67 ± 150.71 MJ m^{-2} yr^{-1}. According to surface energy balance (Equation 7), if the soil heat flux was ignored, the sensible heat flux was 2327.18 ± 334.09 MJ m^{-2} yr^{-1} and the resulting Bowen ratio would be 2.52 ± 0.77, which means that the sensible heat was 2.52 times the latent heat in the Three-River Headwaters in the study period from 2001 to 2018.

The spatial distribution of the Bowen ratio shows it is gradually increasing from the eastern to western region (Fig. 4a). The highest Bowen ratio was found in western Tanggulashan, with an average value of 3.13 and a coefficient of variation of 20.37%; while the southeastern Gander has the

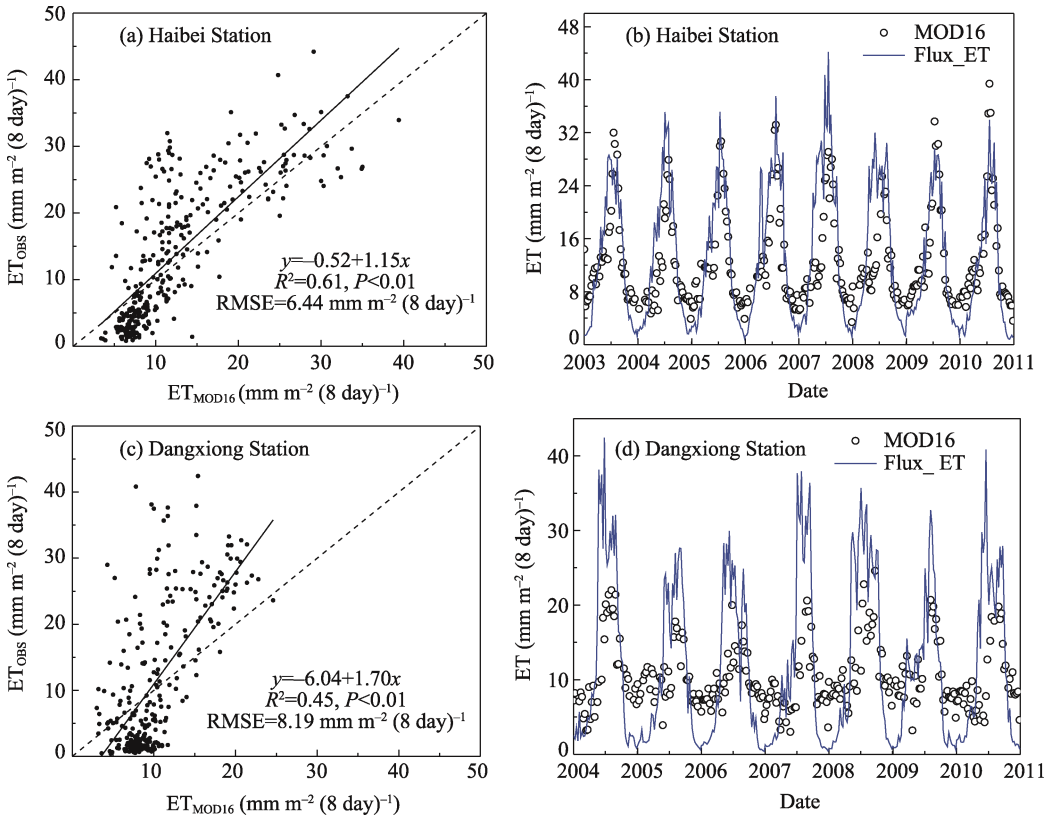

Fig. 3 The evapotranspiration (ET_{MOD16}) products of MODIS (MOD16A2) were validated against the observations (ET_{OBS}) through the linear regression analysis (a, c) and the seasonal change comparisons (b, d) on the alpine grasslands at Haibei Station (a, b) and Dangxiong Station (c, d) on the Qinghai-Tibet Plateau, China.

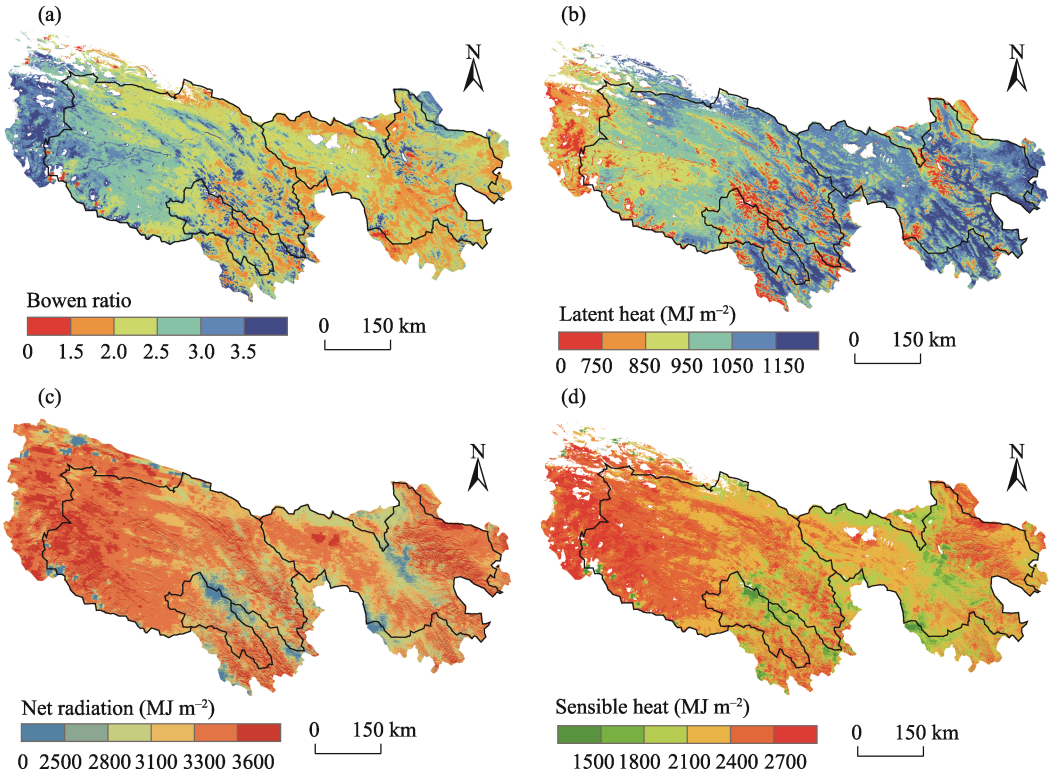

Fig. 4 Distribution patterns of multi-year averages of Bowen ratio (a), Latent heat (b), Net Radiation (c), and Sensible Heat (d) of the Three-River Headwaters from 2001 to 2018.

smallest Bowen, with an average value of 2.00 and a smaller spatial variation with a coefficient of variation of 21.8%.

Among the three basins, the Yellow River has the lowest Bowen ratio, with net radiation of 3271.30±302.37 MJ m^{-2} yr^{-1}, latent heat based on MOD16 products of 1051.41 ± 126.15 MJ m^{-2} yr^{-1}, and sensible heat according to the surface energy balance of 2218.06 ± 279.52 MJ m^{-2} yr^{-1}. Therefore, its Bowen ratio was 2.21 ± 0.35, that is, about 67.80% of the net surface radiation was used to heat the air, while only 32.14% of that was used for vegetation transpiration and soil evaporation.

The net radiation from the Yangtze River source was 3375.44 ± 290.51 MJ m^{-2} yr^{-1}; the latent heat was 945.92 ± 172.92 MJ m^{-2} yr^{-1}, accounting for 28.28% of the net radiation; the sensible heat was 2424.32 ± 284.51 MJ m^{-2} yr^{-1}, accounting for 71.82% of the net radiation; and the Bowen ratio was 2.68 ± 0.30. The net radiation from the Lancang River source was 3168.90 ± 426.34 MJ m^{-2} yr^{-1}, the latent heat was 945.92±172.92 MJ m^{-2} yr^{-1} (29.85% of the net radiation), the sensible heat was 2227.56 ± 365.25 MJ m^{-2} yr^{-1} (70.29% of the net radiation), and the Bowen ratio was 2.55 ± 0.35. The above results of the three basins showed that nearly one-third of the energy is used for the evapotranspiration and that more than two-thirds is used for sensible heat in the whole area, and Yangtze River has the highest Bowen ratio, followed by Lancang River, while the Yellow River has the lowest ratio.

3.3.2 Inter-annual trends of Bowen ratio

According to the linear regression analysis, the Bowen ratio of the whole TRH was significantly decreasing at a rate of –2.5% yr^{-1} (R^2 = 0.21, P = 0.056) in the period from 2001 to 2018. This trend meant that the amount of net surface radiation allocated as sensible heat was decreasing while the amount allocated as latent heat was increasing during the study period, with a confidence level of 94.4% (Fig. 5a). The Bowen ratio of the three basins showed decreasing trends, at a rate of 0.03 per year for the Yellow River basin and 0.02 per year for both the Yangtze and Lancang River basins (Fig. 5b).

The spatial pattern of the Bowen ratio trend showed an increasing trend in 13.57% and a decreasing trend in 72.75% of the area of the whole region (Fig. 6). The increasing trend occurred over the southwestern and central regions, especially in the southeastern Tanggulashan and the western Zaduo, while the decreasing trend occurred over the northeastern region, including Xinghai, Tongde, Zeku and Henan.

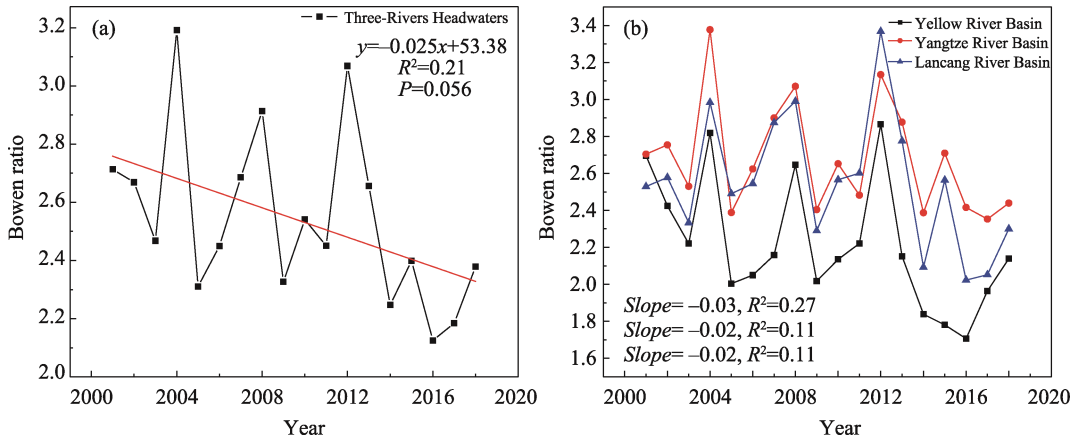

Fig. 5 Inter-annual variation trends of the Bowen ratio in Three-River Headwaters (a) and each of the three sub-Basins (b) from 2001 to 2018

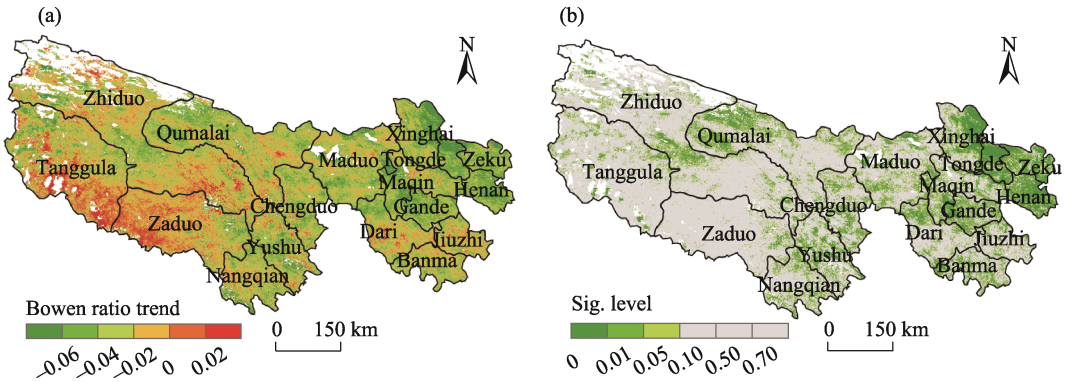

Fig. 6 Spatial pattern of the inter-annual trend of the Bowen ratio (a) and its significant level (b) on the pixel scale for the Three-River Headwaters from 2001 to 2018

3.4 Analysis of the impact factors on the Bowen ratio

3.4.1 Multiple linear regression analysis

Multivariate linear regression analysis was applied to explore the impacts on the Bowen ratio from the climatic factors (P_{AT}, T_{AM}, RH_{AM}), vegetation (N_{AM}) and albedo (A_{AM}), and the results based on the regional mean values are shown in Table 1. With the confidence level of 84%, the five factors can explain 51% of the interannual variation of the Bowen ratio for the whole region, and 57%, 48%, and 46% for the Yellow River Basin, Yangtze River Basin, and Lancang River Basin, respectively, according to the correlation coefficients (R^2). Additionally, the T_{AM}, RH_{AM}, N_{AM} each has a negative effect on the Bowen ratio, while the effects of P_{AT} and A_{AM} varied among the basins according to the standardized regression coefficients. The temperature (T_{AM}) had the greatest effect on the Bowen ratio at the whole regional scale, with a standardized regression coefficient of –0.43, followed by N_{AM} (–0.27), RH_{AM} (–0.14), P_{AT} (–0.08) and A_{AM} (–0.05).

The multiple linear regression was performed at the pixel scale to explore the spatial patterns of the effects of the five factors on the Bowen ratio (Fig. **7**). Over an area of 86% of the whole region, these five factors can explain more than 50% of the variability in the Bowen ratio (Table 2), with the exception of the upstream and valleys of the rivers where the regression with the five factors was insignificant and other unknown factors probably dominate in driving the changes of the Bowen ratio (Fig. 7a, b, Fig. 8).

Among the five factors, the changes in annual mean temperature contributed more than 90% of the variability in the Bowen ratio with the specific contribution rates of 92%, 95% and 118% in the Yellow River, Yangtze River and Lancang River, respectively, and 90% for the whole region. This was followed by the NDVI, with contribution rates of 10.2%, 9.7% and 11.7% for the three basins, respectively. However, the contribution of the humidity was contrasted

Table 1 Multiple linear normalized regression coefficients for the three sub-basins in the Three-River Headwaters and the whole region

Area	b_P	b_T	b_H	b_N	b_A	R^2	P-value
Yellow River	–0.01	–0.55	–0.04	–0.31	–0.09	0.57	0.10
Yangtze River	–0.15	–0.37	–0.19	–0.23	0.02	0.48	0.19
Lancang River	0.02	–0.43	–0.26	–0.22	0.03	0.46	0.23
Whole region	–0.08	–0.43	–0.14	–0.27	–0.05	0.51	0.16

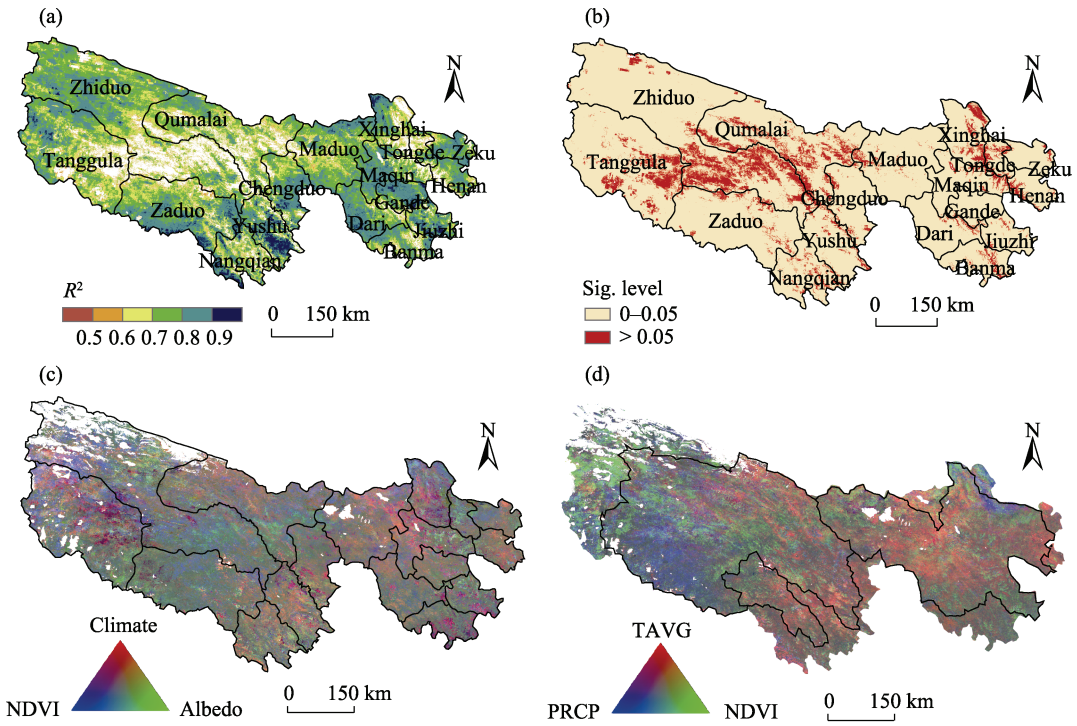

Fig. 7 The trends of Bowen ratio attributed to climate (P_{AT}, T_{AM} and RH_{AM}), vegetation greenness (N_{AM}) and A_{AM} through the multiple linear regression with its multiple correlation coefficient (a), significance level (b), and the regression coefficients multiplied by the trends of the dependent variables (c,d).

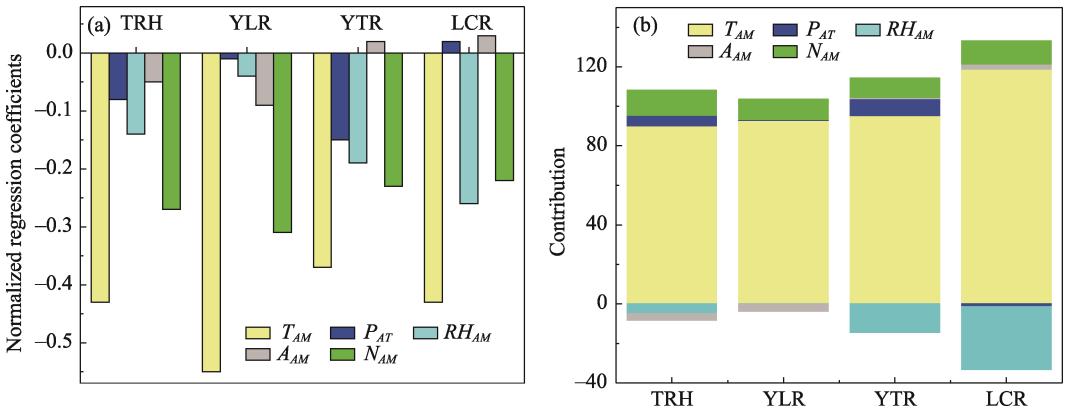

Fig. 8 The standard regression coefficients (a) and their contributions (b) on the Bowen ratio from the annual mean temperature (T_{AM}), annual total precipitation (P_{AT}), annual mean humidity (RH_{AM}), annual mean albedo (A_{AM}) and annual mean normalized difference vegetation index (N_{AM}) in the Three-River Headwaters in the period from 2001 to 2018.

between the two basins of Lancang River (–31.6%) and Yellow River (–0.16%). The contribution of precipitation was less than 10% and varied among the three basins from –1.47% (Lancang), to 0.41% (Yellow) and 8.47% (Yangtze).

The effects of the three types of factors on the spatial pattern varied (Fig. 7b, c). Over the southwestern region, precipitation had the largest influence, but the greatest influence was vegetation status (expressed by NDVI) over the central region, and temperature over the northeastern region.

The Bowen ratio trend was dominated by the increasing air temperature, with a contribution above 90%, which would be attributed to its sensitivity to air temperature and the warming trend in T_{AM}. The Bowen ratio was most sensitive to the interannual variability in the T_{AM} time series (–43%), followed by N_{AM} (–27%) and RH_{AM} (–14%), but was less sensitive to the changes in P_{AT} and A_{AM} (Table 1). On the other hand, the region experienced a significant warming change at the rate of 1.02 ℃ per decade ($P < 0.01$) with an insignificant change in P_{AT}, and the vegetation was greening at the rate of 0.6% per decade ($P = 0.05$) along with its decreasing A_{AM} at the rate of 1% per decade ($P = 0.04$). Therefore, the Bowen ratio showed a decreasing trend induced by temperature (–31.7% per decade), NDVI (–4.5% per decade) and albedo (1.1% per decade) (Table 2).

3.4.2 Analysis by the Structural Equation Model (SEM)

The five key variables were correlated with each other (Fig. 10a). First of all, temperature was significantly and positively correlated with P_{AT} ($R = 0.55$, $P < 0.001$). The N_{AM} was correlated with T_{AM} (0.71), P_{AT} (0.43) and RH_{AM} (0.42). Those correlations among the variables influenced the interannual trend in the Bowen ratio (β). Therefore, the SEM was applied to determine the direct and indirect effects from the above five variables on the Bowen ratio and the results are shown in Fig. 10b and Table 3.

The Bowen ratio was negatively influenced by T_{AM} (–0.53) and RH_{AM} (–0.30), while positively influenced by A_{AM} (0.43). An effect of albedo was not revealed by the MLR, but more information was given by SEM. The A_{AM} was affected by the N_{AM} (–0.57) and RH_{AM} (0.53), and it then played a positive and direct role in influencing the Bowen ratio. The effect of T_{AM} was too strong to be revealed by both methods. P_{AT} directly affected RH_{AM} (0.59) and T_{AM} (0.55), and indirectly affected the Bowen ratio. Furthermore, T_{AM} strongly affected vegetation changes with a path coefficient of 0.72 with N_{AM}. In addition, vegetation changed its A_{AM}, that is, the increasing N_{AM} would result in a decreasing A_{AM} according to the path coefficient of –0.57, and N_{AM} was significantly correlated with A_{AM} ($R^2 = 0.52$, $P < 0.001$), according to the linear regression (Fig. 11). These results meant that the warming climate drove vegetation restoration and both affected the interannual variability in the Bowen ratio by altering the albedo of the insignificant vegetation greening.

Table 2 The 2001–2018 interannual trends of Bowen ratio and related climate variables in the Three-River Headwaters

Region	Area (%)	Bowen trend	T_{AM} trend	P_{AT} trend	RH_{AM} trend	A_{AM} trend	N_{AM} trend	Bowen = $b_T + b_P + b_R + b_A + b_N$					
								b_T	b_P	b_R	b_A	b_N	R^2
TRH	86	–0.0255	0.093(<0.001)	3.88(0.13)	–0.007(0.43)	–0.001(0.07)	0.00047(0.20)	–0.3417	–0.0005	–0.2525	–1.1175	–9.4901	0.5038
YLR	25	–0.0339	0.109(<0.001)	4.71(0.09)	–0.002(0.87)	–0.001(0.16)	0.00059(0.30)	–0.3877	–0.00004	–0.0372	–1.5741	–7.8781	0.5629
YTR	31	–0.0184	0.092(<0.001)	2.40(0.38)	–0.012(0.22)	–0.001(0.04)	0.00031(0.29)	–0.3004	–0.0010	–0.3456	0.2343	–9.0489	0.4715
LCR	4	–0.0204	0.089(<0.001)	1.79(0.62)	–0.026(0.04)	–0.001(0.31)	0.00052(0.33)	–0.3851	0.0002	–0.3506	0.7142	–6.4999	0.4448

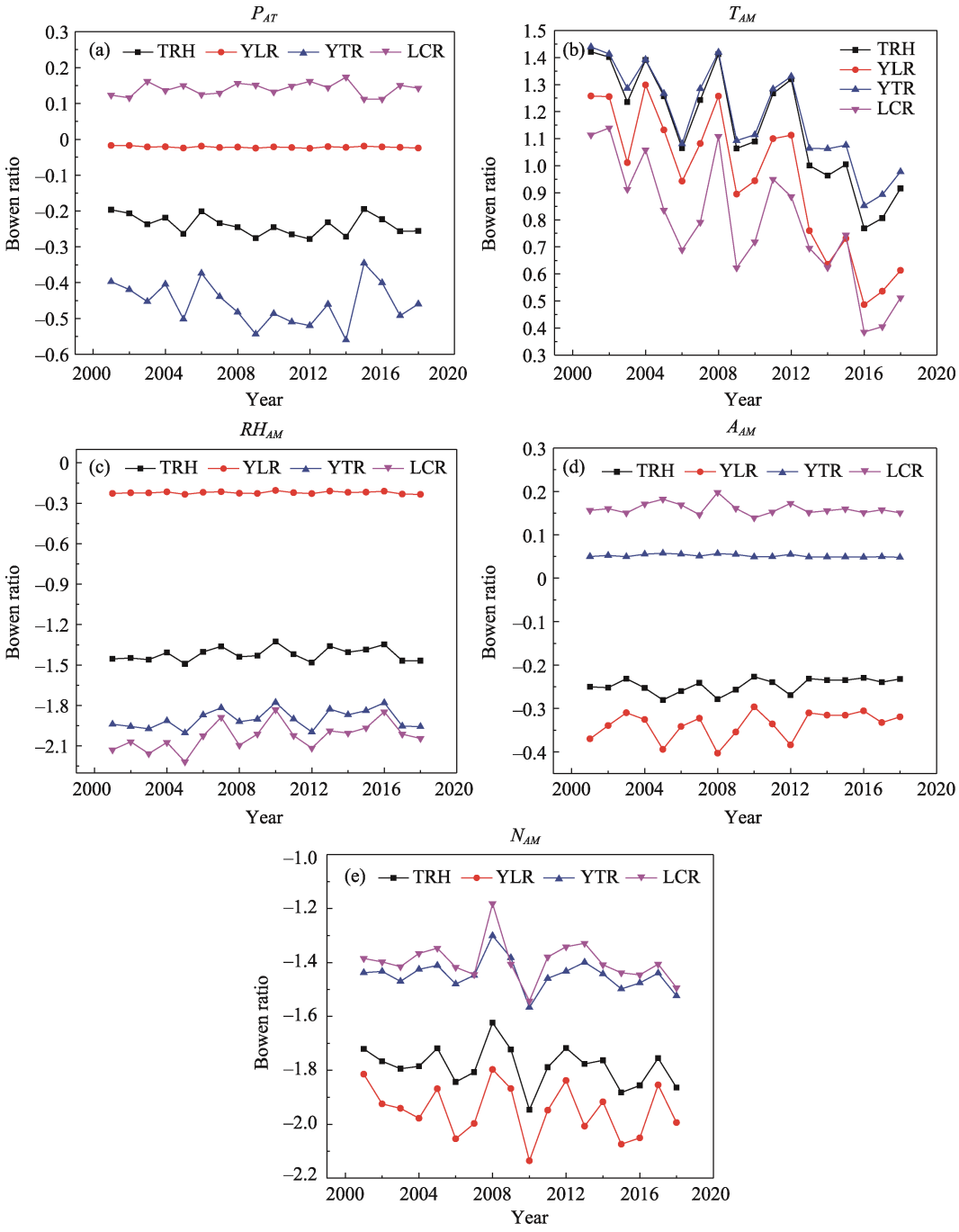

Fig. 9 Effects of different factors on the interannual variation of the Bowen ratio in the Three-River Headwaters: (a) P_{AT}, (b) T_{AM}, (c) RH_{AM}, (d) A_{AM}, and (e) N_{AM}.

Table 3 Fitness test results of SEM

Assessment index	Absolute goodness-of-fit indices							Comparative fit index	Information criteria index
	Chi-sq	*df*	*P* value	RMSEA	SRMR	RMR	GFI	CFI	AIC
Optimal value	$P > 0.05$	–	<0.05	<0.05	<0.08	<0.08	>0.90	>0.90	The smaller, the better
Practical value	0.000	0.000	NA	0.000	0.000	0.000	1.000	1.000	–527.85

Note: Root Mean Square Error of Approximation (RMSEA), Chi-square value (*Chi-sq*), Comparative fit index (CFI), Standardized Root Mean Square Residual (SRMR), Root Mean Square Residual (RMR), Goodness of Fit Index (GFI), Red Pool Information Criterion (AIC). The degree of freedom of the model is 0, so it is called just a recognition model or saturation model, and its chi-square value is also 0. All parameters of this model have only unique solutions. A CFI of 1 means that the model is fully adapted.

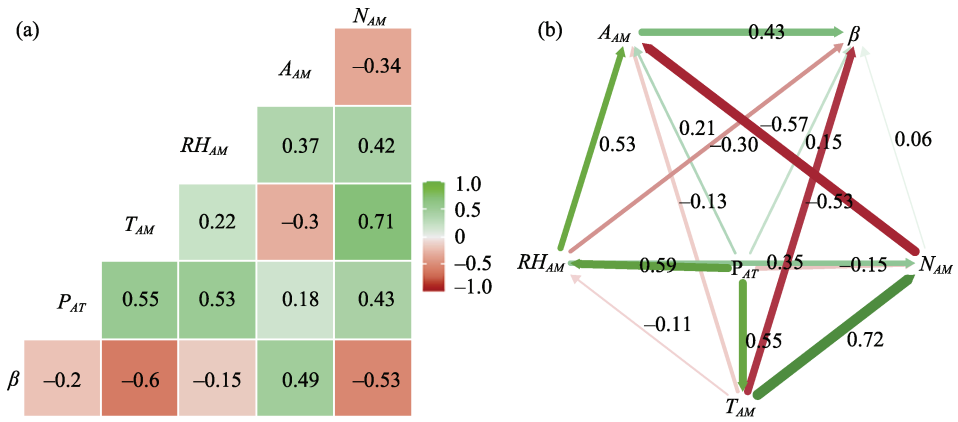

Fig. 10 The correlation matrix (a) and the structural equation model (b) for the variables of annual total precipitation (P_{AT}), the annual mean temperature (T_{AM}), annual mean relative humidity (RH_{AM}), and the vegetation factors of the annual mean Albedo (A_{AM}) and annual mean normalized difference vegetation index (N_{AM}), and the Bowen ratio (β).

Note: In subplot (b), the width of a line indicates the correlation and the green and red colors indicate a positive and a negative effect, respectively. The labeled values are the normalized path coefficients.

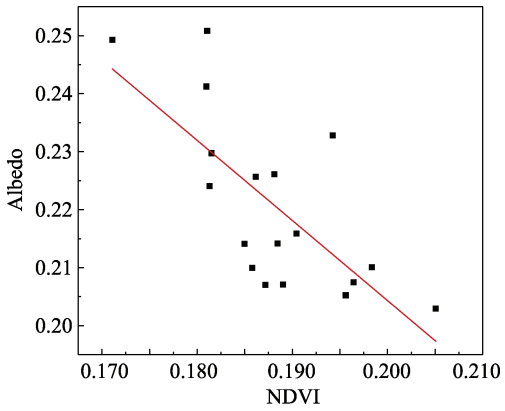

Fig. 11 The annual mean albedo was significantly correlated with the annual mean NDVI in the Three-River Headwaters, Qinghai Province, in the period from 2001 to 2018.

4 Discussion

4.1 Uncertainty in the Bowen ratio calculation

In this study, the Bowen ratio was calculated from the remote sensing-based evapotranspiration (ET) data from the MODIS product (MOD16 V006). Therefore, the uncertainty mainly came from the MOD16 data. Here the product (ET_{MODIS}) was validated against the ET (ET_{OBS}) which was estimated from the latent heat data observed on the eddy covariance towers in the alpine grassland. As the validation showed, the MOD16 data were significantly well-correlated with the observations. However, the MOD16 could only explain 45% and 61% of the variability in the observations in the two alpine grassland sites of Dangxiong and Haibei on the Qinghai-Tibet Plateau, respectively. The uncertainties, however, probably came from the observations since the eddy covariance technique is considered to be the standard method for determining energy and substance fluxes (Tian et al., 2006). Despite advances in the development and improvement of instrumentation, energy balance closure is a problem which persists (Li et al., 2004). On the other hand, there are some uncertainties in the MOD16 products which arise from its algorithm and the input data; so the algorithm should be further improved, especially the soil water balance estimation which was not considered in the most recent ET algorithm (Yan et al., 2012). In the future, more flux sites should be applied to improve the ET algorithm by considering surface energy balance through the optimization of the parameters.

4.2 Factors affecting the inter-annual variation of the Bowen ratio

As the ratio of sensible heat (H) to latent heat (λET) in Equation 6, the Bowen ratio is affected by climate, vegetation and soil properties (Monteith and Unsworth, 2013; Tang et al., 2014). Previous studies have reported that the Bowen ratio was affected by soil moisture through the water supply for surface evaporation (Wang et al., 2003; Zhao et al., 2008), by surface roughness through changes in the aerodynamic impedance (Pitman, 2003), and by the freeze-thaw cycle (Ge et al., 2016). However, in this study, temperature was found to be the dominant factor along with humidity and albedo as the secondary factors, which was also found in a sub-tropical forest (Tang et al., 2014). Temperature plays a dominant role because it is one of important factors controlling the many physiological and chemical reaction processes in ecosystems and it acts as a regulator and allocator of energy, water and nutrients in ecosystems (Yu and Xu, 2009; Yao and Zhang, 2015). Humidity has a strong influence on vegetation growth and production, as well as biological diversity in arid and semi-arid regions (Ye et al., 2012). Vegetation factors, here represented by NDVI, seem have no effect on the Bowen ratio, and in fact, through altering albedo to affect the Bowen ratio, such interactions were well quantified by the SEM analysis (Fig. 9b).

4.3 Importance and aspects for further study

Land use and cover change, such as planting, grazing, deforestation and afforestation, was considered as one of the important drivers of climate by altering surface energy balance (Turner et al., 1995; Li, 1996; Pitman, 2003). Alpine grasslands have experienced degradation since the early 1970s and restoration since 2005 (Liu et al., 2008; Shao et al., 2013; Shao et al., 2017; Huang et al., 2018), which has probably resulted in the changes of surface energy balance, known as the biogeophysical effect (Zhao et al., 2019). On the interannual scale, the Bowen ratio showed a decreasing trend for the warming climate changes in the background of global warming, and a decreasing albedo due to vegetation restoration as shown by the increasing NDVI (Fig. 2). A decreasing Bowen ratio, that is, an increasing latent heat or a decreasing sensible heat, will inhibit the warming effect of the surface on the atmosphere. In this sense, the Bowen ratio could be applied to assess ecosystem quality as an indicator of the regulating function of the ecosystem.

5 Conclusions

In this paper, the Bowen ratio was calculated from the evapotranspiration products of MODIS (MOD16) and its interannual trends and affecting factors were analyzed in the Three-River Headwaters region of China over the period of 2001–2018. The Bowen ratio was found to have a trend of decreasing by 25% per decade, which was mainly attributed to a warming climate, changing humidity and greening vegetation. Specifically, a changing climate dominated by global warming, superimposed on slightly increasing precipitation, will promote vegetation growth and a decreasing surface albedo, leading to an increasing net surface radiation; but at the same time, climate warming dominates and directly contributes to increased surface evapotranspiration, leading to a decrease in the Bowen ratio. However, the validation of the data from MOD16 indicated that its algorithm has some room for improvement. It is essential to develop a new algorithm and improve the accuracy of latent and sensible heat estimations by the fusion of the ecosystem process model and observations from more eddy covariance towers. This study expands our understanding of the biogeophyscial effects of grassland restoration as one type of land use and cover change, and provides a knowledge foundation for using the Bowen ratio as an indicator of the climate regulating function of ecosystem assessments in future.

References

Bastiaanssen W G M. 2000. SEBAL-based sensible and latent heat fluxes in the irrigated Gediz Basin, Turkey. *Journal of Hydrology*, 229(1–2): 87–100.

Betts R A. 2000. Offset of the potential carbon sink from boreal forestation by decreases in surface albedo. *Nature*, 408(6809): 187–190.

Bonan G B. 2008. Forests and climate change: Forcings, feedbacks, and the climate benefits of forests. *Science*, 320(5882): 1444–1449.

Bonan G B. 2017. Ecoclimatology concepts and applications (2nd ed.). Beijing, China: Meteorological Press.

Bowen I S. 1926. The ratio of heat losses by conduction and by evaporation from any water surface. *Physical Review*, 27: 779–787.

Cao M K, Li K R. 2000. Perspective on terrestrial ecosystem-climate interaction. *Advance in Earth Sciences*, 15(4): 446–452. (in Chinese)

Cui M Y, Wang J B, Wang S Q, et al. 2019. Temporal and spatial distribution of evapotranspiration and its influencing factors on Qinghai-Tibet Plateau from 1982 to 2014. *Journal of Resources and Ecology*, 10(2): 213–224.

Dugas W A, Fritschen L J, Gay L W, et al. 1991. Bowen ratio, eddy correlation, and portable chamber measurements of sensible and latent heat flux over irrigated spring wheat. *Agricultural and Forest Meteorology*, 56(1–2): 1–20.

Feddema J J, Oleson K W, Bonan G B, et al. 2005. The importance of land-cover change in simulating future climates. *Science*, 310(5754): 1674–1678.

Ge J, Yu Y, Li Z C, et al. 2016. Impacts of freeze/thaw processes on land surface energy fluxes in the permafrost region of Qinghai-Xizang Plateau. *Plateau Meteorology*, 35(3): 608–620. (in Chinese)

Geli H M, Taghvaeian S, Neale C M, et al. 2010. Estimation of evapotraspiration of tamarisk using energy balance models with high resolution airborne imagery and LIDAR data. San Francisco, USA: AGU Fall Meeting Abstracts.

Hao X C, Zhang Q, Yang Z S, et al. 2016. A new method for drought monitoring based on land surface energy balance and its preliminary application to the Hedong region of Gansu Province. *Chinese Journal of Geophysics*, 59(5): 488–503.

Hua K T, Cheng Z J. 1999. Application and analytical strategies of structural equation modelling. *Exploration of Psychology*, 19(1): 54–59. (in Chinese)

Huang B R, Wang Y, Su L Y, et al. 2018. Pilot programs for national park system in China: Progress, problems and recommendations. *Bulletin of Chinese Academy of Sciences*, 33: 76–85. (in Chinese)

Hutchinson M F. 1991. The application of thin plate splines to continent wide data assimilation, Data Assimilation Systems. In: Jasper J D (ed.). Data assimilation systems. Melboure, Australia: BMRC Research Report.

Hutchinson M F. 1998a. Interpolation of rainfall data with Thin Plate Smoothing Splines. Part I: Two dimensional smoothing of data with short range correlation. *Journal of Geographic Information and Decision Analysis*, 2: 153–167.

Hutchinson M F. 1998b. Interpolation of rainfall data with Thin Plate Smoothing Splines. Part II: Analysis of topographic dependence. *Journal of Geographic Information and Decision Analysis*, 2: 168–185.

Jönsson P, Eklundh L. 2004. TIMESAT—A program for analyzing time-series of satellite sensor data. *Computers & Geosciences*, 30(8): 833–845.

Li X B. 1996. Core areas of global environmental change research: International trends in land use/land cover change. *Acta Geographica Sinica*, 51(6): 553–558. (in Chinese)

Li Z Q, Yu G R, Wen X F, et al. 2004. Evaluation of the closed state of the energy balance of China FLUX. *Science in China* (*Serires D*), 34(S2): 46–56. (in Chinese)

Liu C C, Liu G R, Chen W J, et al. 2003. Modified Bowen ratio method in

near-sea-surface air temperature estimation by using satellite data. *IEEE Transactions on Geoscience and Remote Sensing*, 41(5): 1025–1033.

Liu J Y, Xu X L, Shao Q Q. 2008. The spatial and temporal characteristics of grassland degradation in the Three-River Headwaters region in Qinghai Province. *Acta Geographica Sinica*, 63(4): 364–376. (in Chinese)

Liu N F, Liu Q, Wang L Z, et al. 2013a. A statistics-based temporal filter algorithm to map spatiotemporally continuous shortwave albedo from MODIS data. *Hydrology and Earth System Sciences*, 17(6): 2121–2129.

Liu Q, Wang L Z, Qu Y, et al. 2013b. Preliminary evaluation of the long-term GLASS albedo product. *International Journal of Digital Earth*, 6(S1): 69–95.

McDonald R P, Ho M H R. 2002. Principles and practice in reporting structural equation analyses. *Psychological Methods*, 7(1): 64–82.

Mei Q. 2000. Three-River Headwaters: A great leap for China's ecological protection cause. *Forestry of China*, (9): 4–5. (in Chinese)

Monteith J L, Unsworth M H. 2013. Transient heat balance (Chapter 15). In: Jeanne L, Lori A, André A C (eds.). Principles of environmental physics (4th ed.). Boston, USA: Academic Press, 273–287.

Mu Q Z, Heinsch F A, Zhao M, et al. 2007. Development of a global evapotranspiration algorithm based on MODIS and global meteorology data. *Remote Sensing of Environment*, 111(4): 519–536.

Mu Q Z, Zhao M, Running S W. 2011. Improvements to a MODIS global terrestrial evapotranspiration algorithm. *Remote Sensing of Environment*, 115(8): 1781–1800.

Pielke R A, Marland G, Betts R A, et al. 2002. The influence of land-use change and landscape dynamics on the climate system: Relevance to climate-change policy beyond the radiative effect of greenhouse gases. *Philosophical Transactions of the Royal Society* (*Series A*), 360(1797): 1705–1719.

Pitman A J. 2003. The evolution of, and revolution in, land surface schemes designed for climate models. *International Journal of Climatology*, 23(5): 479–510.

Qu Y, Liu Q, Liang S, et al. 2014. Direct-estimation algorithm for mapping daily land-surface broadband albedo from MODIS data. *IEEE Transactions on Geoscience and Remote Sensing*, 52(2): 907–919.

Rosseel Y. 2012. Lavaan: An R package for structural equation modeling. *Journal of Statistical Software*, 48(2): 1–36.

Shao Q Q, Fan J W. 2012. Comprehensive monitoring and assessment of ecosystems in Three-Rivers Headwaters. Beijing, China: Science Press. (in Chinese)

Shao Q Q, Fan J W, Liu J Y, et al. 2017. Target-based assessment on effects of first-stage ecological conservation and restoration project in Three-river Source Region, China and policy recommendations. *Bulletin of Chinese Academy of Sciences*, 32: 35–44. (in Chinese)

Shao Q Q, Liu J Y, Huang L, et al. 2013. Integrated assessment on the effectiveness of ecological conservation in Sanjiangyuan National Nature Reserve. *Geographical Research*, 32(9): 1645–1656. (in Chinese)

Shipley B. 2000. A new inferential test for path models based on directed acyclic graphs. *Structural Equation Modeling*: *A Multidisciplinary Journal*, 7(2): 206–218.

Tang Y K, Wen X F, Sun X M, et al. 2014. Interannual variation of the Bowen ratio in a subtropical coniferous plantation in southeast China, 2003–2012. *Plos One*, 9(2): e88267. DOI: 10.1371/journal.pone.0088267.

Tian J, Zhang R H, Sun X M, et al. 2006. Study on the correction model of the influence of horizontal advection flow observation based on remote sensing information. *Science in China* (*Series D*), (1): 255–262. (in Chinese)

Turner B L, Skole D, Sanderson S, et al. 1995. Land-use and land-cover change: Science/research plan. Stockholm, Sweden: International Geosphere-Biosphere Programme.

Wang G X, Shen Y P, Qian J, et al. 2003. Study on the influence of vegetation changeon soil moisture cycle in alpine meadow. *Journal of Glaciology and Geocryology*, 25(6): 653–659. (in Chinese)

Wang J B. 2007. Modeling carbon fluxes of terrestrial ecosystem on regional scale through coupling a remote sensing model with an ecosystem process model. Diss., Beijing, China: Institute of Geographic Sciences and Natural Resources Research, Chinese Academy of Sciences. (in Chinese)

Wang J B, Wang J W, Ye H, et al. 2017. An interpolated temperature and precipitation dataset at 1-km grid resolution in China (2000–2012). *Science Data Bank*, 2: 73–80. (in Chinese)

Wang L M, Lee X, Schultz N, et al. 2018. Response of surface temperature to afforestation in the Kubuqi Desert, Inner Mongolia. *Journal of Geophysical Research*: *Atmospheres*, 123(2): 948–964.

Wang S Q, Wang J B, Zhang L M, et al. 2019. A National Key R&D Program: Technologies and guidelines for monitoring ecological quality of terrestrial ecosystems in China. *Journal of Resources and Ecology,* 10(2): 105–111.

Wang Z, Wang J B. 2019. Changes of soil erosion and possible impacts from ecosystem recovery in the Three-River Headwaters region, Qinghai, China from 2000 to 2015. *Journal of Resources and Ecology*, 10(5): 461–471.

Yan H, Wang S Q, Billesbach D, et al. 2012. Global estimation of evapotranspiration using a leaf area index-based surface energy and water balance model. *Remote Sensing of Environment*, 124: 581–595.

Yang Y H, Wang J B, Liu P, et al. 2019. Climatic changes dominant interannual trend in net primary productivity of alpine vulnerable ecosystems. *Journal of Resources and Ecology*, 10(4): 379–388.

Yao Y H, Zhang B P. 2015. The spatial pattern of monthly air temperature of the Tibetan Plateau and its implications for the geo-ecology pattern of the Plateau. *Geographical Research*, 34(11): 2084–2094. (in Chinese)

Ye H, Wang J B, Huang M, et al. 2012. Spatial pattern of vegetation precipitation use efficiency and its response to precipitation and temperature on the Qinghai-Xizang Plateau of China. *Chinese Journal of Plant Ecology*, 36(12): 1237–1247. (in Chinese)

Yu G R, Wen X F, Sun X M, et al. 2006. Overview of ChinaFLUX and evaluation of its eddy covariance measurement. *Agricultural and Forest Meteorology*, 137: 125–137.

Yu G R, Zhang L M, Sun X M, et al. 2008. Environmental controls over carbon exchange of three forest ecosystems in eastern China. *Global Change Biology*, 14(11): 2555–2571.

Yu G R, Chen Z, Piao S L, et al. 2014. High carbon dioxide uptake by subtropical forest ecosystems in the East Asian monsoon region. *Proceedings of the National Academy of Sciences of the USA*, 1111(13): 4910–4915.

Yu H Y, Xu J C. 2009. Effects of climate change on vegetations on Qinghai-Tibet Plateau: A review. *Chinese Journal of Ecology*, 28(4): 747–754. (in Chinese)

Zhang X, Liu X Q, Zhang L F, et al. 2017. Energy balance of an artificial

grassland in the Three-River Source Region of the Qinghai-Tibet Plateau. *Acta Ecologica Sinica*, 37(15): 4973–4983. (in Chinese)

Zhang Z S, Zhao A G, Dong Z B. 2006. Measurement of ecosystem surface flux: Introduction of multi-channel Bowen ratio measuring instrument. *Journal of Desert Research*, 26(3): 473–477. (in Chinese)

Zhao G S, Dong J W, Cui Y P, et al. 2019. Evapotranspiration-dominated biogeophysical warming effect of urbanization in the Beijing-Tianjin-Hebei region, China. *Climate Dynamics*, 52(1–2): 1231–1245.

Zhao S X, Zhang Y S, Zhao X Q, et al. 2008. Research on evapotranspiration and its impact factors on grassland in the northern slopes of Qilianshan Mountains. *Journal of Northwest A & F University* (*Natural Science Edition*), (1): 109–115. (in Chinese)

Zhao W, Li A N. 2015. A review on land surface processes modelling over complex terrain. *Advances in Meteorology*, 2015: 607181. DOI: 10.1155/2015/607181.

Zhu Z C, Bi J, Pan Y Z, et al. 2013. Global data sets of vegetation Leaf Area Index (LAI) 3g and Fraction of Photosynthetically Active Radiation (FPAR) 3g derived from Global Inventory Modeling and Mapping Studies (GIMMS) Normalized Difference Vegetation Index (NDVI3g) for the period 1981 to 2011. *Remote Sensing*, 5(2): 927–948.

2001–2018 年青藏高原三江源地区高寒草地的波文比

赵烜岚[1,2]，王军邦[1]，叶　辉[3]，MUHAMMAD Amir[1,2]，王绍强[1]

1. 中国科学院地理科学与资源研究所 生态系统网络观测与模拟重点实验室 国家生态系统科学数据中心，北京 100101；
2. 中国科学院大学，北京 100049；
3. 九江学院旅游与地理学院，江西九江 332005

摘　要：波文比用以描述从地球表面到空气中以潜热或感热发生的热传递过程，其由于土地利用和覆盖变化的生物物理效应而成为研究热点。波文比对评估生态系统气候调节功能具有一定的作用，但在大多数生态评估中常常被忽略。本文以位于气候敏感区和脆弱区的青藏高原腹地的三江源地区为研究区域，基于 MODIS 蒸散产品以及 2001–2018 年 MODIS 反照率计算出的陆地表面净辐射估算出波文比，并利用通量观测数据对 MODIS 蒸散产品进行了验证。通过多元线性回归和结构方程模型（SEM）两种方法分别分析了波文比的时空变化和影响因素。结果表明：1）MOD16 蒸散数据与海北和当雄两个高寒草甸的涡度通量观测数据显著相关，相关系数分别为 0.78 和 0.70，显著水平 P 值均小于 0.01；2）2001–2018 年期间三江源地区草地的多年平均波文比是 2.52 ± 0.77，呈从东南向西北逐渐递增的空间格局；研究时段内波文比整体呈下降趋势（$Slope = -0.025$, $R^2 = 0.21$, $P = 0.056$）；3）以年总降水量、年平均气温、年平均相对湿度、年平均 NDVI 及年均反照率为自变量的多元线性回归方程，可解释三江源全区平均波文比年际变化的 51%，根据标准化回归系数，气温的影响最大，这表明气候变暖对净辐射分配为感热和潜热的比例有很大的影响；4）此外，植被变化的贡献通过结构方程模型进行定量分析，结果表明 NDVI 的增加将导致反照率的下降，路径系数为–0.57，反照率对波文比影响为正，路径系数为 0.43，这是由于气候变化引起的 NDVI 变化的负面和间接影响。明显的湿润气候可以增加蒸散，以全球气候变暖为主并叠加降水增加的气候变化，将促进植被生长，地表反照率降低，会使地表净辐射增加；但同时气候变暖主导并直接促进了地表蒸散增加，导致了波文比降低，表明波文比能够综合反映区域气候和植被变化的生物地球物理效应，可在今后生态系统评估中作为气候调节功能指标之一。

关键词：高寒草地；波文比；三江源；MODIS；蒸散